ELSEVIER

Journal of Nuclear Materials 281 (2000) 42–56

journal of nuclear materials

www.elsevier.nl/locate/jnucmat

Quantitative analysis of deuterium in a-C:D layers, a Round Robin experiment

R. Behrisch [a,*], M. Mayer [a], W. Jacob [a], W. Assmann [b], G. Dollinger [c], A. Bergmaier [c], U. Kreissig [d], M. Friedrich [d], G.Y. Sun [d], D. Hildebrandt [e], M. Akbi [e], W. Schneider [e], D. Schleußner [f], W. Knapp [f], C. Edelmann [f]

[a] *Max-Planck-Institut für Plasmaphysik, Euratom Association, Boltzmanstrasse 2, D-85748 Garching, Germany*
[b] *Sektion Physik, Ludwig-Maximilians-Universität München, D-85748 Garching, Germany*
[c] *Physik Department E12, Technische Universität München, D-85748 Garching, Germany*
[d] *Institut für Ionenstrahlphysik und Materialforschung, Forschungszentrum Rossendorf, POB 510119, D-01314 Dresden, Germany*
[e] *Max-Planck-Institut für Plasmaphysik, Euratom Association, Bereich Berlin, D-10117 Berlin, Germany*
[f] *Institut für Experimentelle Physik, Abteilung Vakuumphysik und-technik, Otto-von-Guericke-Universität Magdeburg, POB 4120, D-39016 Magdeburg, Germany*

Received 22 November 1999; accepted 13 May 2000

Abstract

The absolute amount of deuterium in amorphous deuterated carbon (a-C:D) layers has been measured by six laboratories with different techniques, such as MeV ion beam analysis, secondary ion mass spectrometry (SIMS), and thermal desorption spectrometry (TDS). The a-C:D layers have been deposited from a CD_4 glow discharge plasma onto carbon and silicon substrates. The results for the absolute numbers obtained with the different analysing techniques show a scatter of up to about 35% around the average value. These deviations are larger than the errors stated by the experimentalists and indicate possible systematic uncertainties in some of the measurements.

1. Introduction

In experiments with magnetically confined high temperature hydrogen plasmas such as investigated in controlled thermonuclear fusion research, the vessel walls are bombarded with hydrogen isotope ions and energetic neutral atoms at energies ranging from a few eV to keV [1–4]. This causes implantation and accumulation of hydrogen isotopes in the plasma facing wall materials [5–9]. For an understanding and control of the hydrogen balance and tritium inventory in fusion experiments, it is important to be able to quantitatively analyse the total amount of hydrogen isotopes in different areas of the vessel walls, and to get information on the depth distributions and binding states of the hydrogen trapped in the wall materials. The quantitative analysis of hydrogen isotopes in thin films is also of significant importance beyond the field of fusion research. For example, the properties of amorphous hydrogenated carbon (a-C:H) layers depend to a large extent on the hydrogen content [10,11]. Such films are usually produced from low-pressure glow discharges in hydrocarbon gases and their hydrogen content may vary over wide ranges depending on the deposition conditions [10–14]. In addition, hydrogen plays an important role in the microstructure of other amorphous hydrogenated materials, such as e.g. amorphous hydrogenated boron (a-B:H) [15] and silicon (a-Si:H) layers [16]. The quantitative determination of the hydrogen content is an important prerequisite for the understanding of the microscopic structure of these materials.

* Corresponding author. Tel.: +49-89 3299 1250; fax: +49-89 3299 1212.
E-mail address: reb@ipp.mpg.de (R. Behrisch).

0022-3115/00/$ - see front matter
PII: S0022-3115(00)00069-6

Several analysis techniques can be applied for measuring the total amount and the depth distribution of deuterium in the surface layers of solids [17–19]. These are MeV ion beam analysis techniques [20], such as nuclear reaction analysis (NRA) [15–21], proton elastic backscattering [22] and elastic recoil detection analysis (ERDA) [15,19,23–27], sputter depth profiling with calibrated secondary ion mass spectrometry (SIMS) [28], including accelerator mass spectrometry (AMS) for tritium analysis [29,30], and thermal desorption spectrometry (TDS) [31]. All these techniques give in principle quantitative results. The MeV ion beam techniques can give directly absolute numbers if the analysing ion fluences and the opening angles of the detectors are known, while for SIMS, AMS and TDS calibrations are necessary.

In sputter depth profiling, such as calibrated SIMS [28] and AMS [29,30], the hydrogen isotopes in surface layers up to a depth of several 10 μm are probed with very high sensitivity, while in TDS [31], the hydrogen isotopes trapped not only in the surface layer, but also in the bulk of the material, are measured. With the SIMS and TDS techniques, the analysed layers of the samples are destroyed during the measurement. In MeV ion beam analysis only surface layers of typically <1 μm are analysed [32] and only some destruction takes place, such as dislocation of atoms by the incident ion beam and loss of volatile species. This has to be taken into account in evaluating the measured data [33–35].

With the $D(^3He,p)\alpha$ NRA technique, using ^3He ions with energies of 790 keV, depths of about 1 μm can be probed [18,19]. Larger depths up to several μm have been analysed using higher incident ^3He energies up to 2.6 MeV [18,36,37], or cutting the surface layer at an oblique angle, such as in ion beam slope cutting (IBSC), and analysing the surface of the slope with a microbeam [21,38]. Deuterium can further be measured with proton elastic backscattering [22,39,40]. However, for incident proton energies of 2.5 MeV, the analysed depth is also limited to about 1 μm and the deuterium signal overlaps with the high intensity of protons backscattered from the substrate material, resulting in additional statistical errors. In ERDA, using primary heavy ions with energies in the MeV per atomic mass unit (amu) range, all hydrogen isotopes and their depth distributions as well as the surface layer chemical composition are measured up to the μm range [25–27,32].

In this work, the MeV ion beam techniques NRA and ERDA with incident He ions and heavy ions, sputter depth profiling with SIMS and TDS have been applied in several different laboratories for the analysis of a-C:D films. The films have been deposited in one deposition run from a low-pressure glow discharge in CD_4 onto polished graphite and silicon substrates. All the a-C:D films on the C and Si samples were thoroughly analysed by NRA prior to shipment to the different groups in order to ensure the same deposition on each sample.

2. Sample preparation

20 graphite and 25 silicon samples were simultaneously coated with an a-C:D layer. The samples were labelled by a number and material according to Fig. 1. The carbon samples were numbered from 21C to 40C, the silicon samples from 1Si to 25Si. The carbon samples ($10 \times 10 \times 3$ mm^3 in size) were machined from fine grain graphite EK98 and mechanically polished on one side. The remaining surface roughness, including cracks was in the μm range. They were cleaned several times in an ultrasonic bath of isopropanol and subsequently degassed for 4 h in a vacuum of about 1×10^{-5} mbar at a temperature of 900°C. The single-crystalline silicon samples (about $10 \times 10 \times 0.4$ mm^3 in size) were also cleaned in an ultrasonic bath using isopropanol, acetone, and distilled water for 10 min each.

The 20 graphite samples were fastened in the central area of a stainless steel electrode having a diameter of 10 cm (Fig. 1). Differences in height relative to the surface of the electrode and between the samples would cause inhomogeneities and fringes during plasma deposition. In order to avoid these steps, grooves have been machined in the stainless steel electrode which allowed to position the surface of the graphite samples at the same level as the remainder of the electrode surface so that no steps or elevations occurred. Inhomogeneities are also caused by distortions of the electric fields due to the transition from one to another material. In order to reduce these fringe effects the carbon samples were mounted in a rectangular area consisting of five columns and four rows with the sides pressed close to each other. In this arrangement four samples at the corners of this rectangle (samples no. 21C, 25C, 36C, and 40C, see Fig. 1) have a neighbouring stainless steel surface on two sides. The 10 samples at the sides of the rectangle border have a stainless steel surface on one side and only the six central samples have just adjacent graphite surfaces. Although we assume that the transition from steel to graphite does not induce significant deviations of the thickness and composition of the deposited film, the four samples from the corner positions were not used for the Round Robin analysis. Since the samples are pressed together from the sides, it is also assured that only the plasma-facing surface of each graphite sample is coated with the film. This is especially important for the TDS analyses in order to avoid coatings on the sides of the substrates, which would contribute to the signal. The deposition rate and the structure, especially the hydrogen or deuterium content, respectively, of a-C:H or a-C:D films depend further on the substrate temperature [14,41]. For a homogeneous deposition all samples must

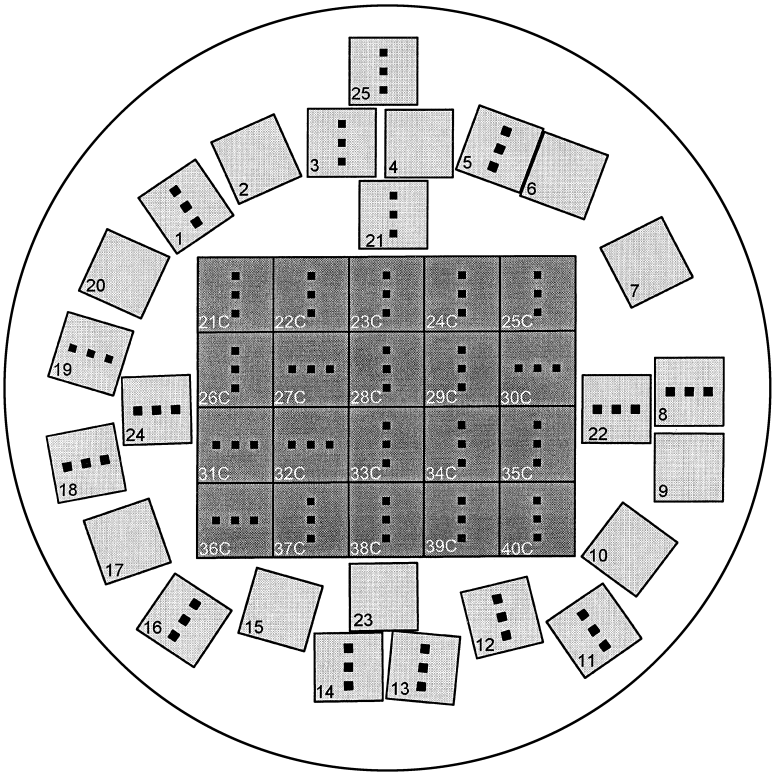

Fig. 1. Positions of the samples on the sample holder during the plasma deposition of the a-C:D layers. The inner 5×4 block shows the positions of the 20 carbon samples. The 25 silicon samples were placed without clamping on the outer ring of the stainless steel substrate holder. The squared spots on the samples indicate the positions of the NRA analysis performed prior to shipping.

have approximately the same temperature. This was achieved for the carbon samples by the tight mounting of the 5×4 samples.

20 silicon samples were placed on the stainless steel electrode in a circle around the centrally arranged carbon samples and at a distance of about 1 cm from the rim (samples no. 1Si–20Si, see Fig. 1). Five silicon samples (samples no. 21Si–25Si) were placed at other positions to allow an estimation of the overall homogeneity. The silicon samples could not be clamped very tightly to the substrate holder; therefore, a larger temperature variation causing a variation of the film thickness and stoichiometry among the silicon samples cannot be excluded. Investigations of the temperature dependence of the a-C:H film deposition in the same set-up have shown that up to deposition temperatures of about 500 K the film stoichiometry and deposition rate are practically independent of temperature [42]. The deposition temperature was actually not measured explicitly but, based on previous experience, it can be assumed that it was well below 400 K. Therefore no large temperature-induced difference between the depositions on the silicon and carbon samples is anticipated. In spite of this, a lower total deuterium content was found on the silicon samples compared with the carbon samples, see Section 3.1.

The amorphous deuterated carbon films (a-C:D) were deposited from a capacitively coupled 13.56 MHz radio-frequency glow discharge plasma, using CD_4 as precursor gas. A detailed description of the deposition apparatus is given elsewhere [43]. Prior to deposition, the substrates were cleaned in a hydrogen discharge for 25 min at a pressure of 2 Pa, an applied power of 90 W (power density 1.2 W cm^{-2}), and a dc self-bias voltage of −350 V. Film deposition was carried out at a pressure of 10 Pa, an applied power of 40 W (power density 0.5 W cm^{-2}), and a dc self-bias voltage of −150 V. The precursor gas was research grade CD_4 with a nominal purity of 99.0% (the main specified impurity is CD_xH_y, $x + y = 4$), but mass spectrometric analysis revealed an impurity concentration of 3.1% N_2. This did, however, pose no problem for the present experiments, because the major aim was to produce several samples with a carbon surface layer containing a well defined amount of deuterium. In the ERDA measurement up to 0.3 at.% of N have been found throughout the deposited layers. The etching and deposition parameters for the a-C:D layers are summarised in Table 1.

Table 1
Parameters for the plasma deposition of the a-C:D layers and substrate cleaning

Parameter	Film deposition	Cleaning step
Precursor gas	CD_4	H_2
Gas flow (cm^3 NTP)	5	20
Gas pressure (Pa)	10	2
RF power density (W cm^{-2})	0.5	1.5
DC self-bias (V)	−150	−350
Substrate temperature (K)	<320	<320

Usually, good film homogeneity is achieved with this set-up for a single wafer up to 10 cm in diameter. Significant film thickness variations are in general restricted to a ring of about 0.5 cm from the rim of the substrate holder. The film thickness of the coated silicon samples was determined using a profilometer (Tencor Alpha Step 200). The thickness of the 20 silicon samples placed in the ring (samples no. 1Si to 20Si) was very homogeneous, in agreement with the optical inspection of the interference colour. For all 20 samples a small thickness gradient of about 2% was measured. The average thickness on the sample site closer to the centre of the electrode is (301 ± 2) nm and it is (294 ± 2) nm on the site closer to the rim. The thickness gradient over a distance of about 3 cm is given by comparison of the thickness measurements on samples 21Si, 3Si, and 25Si. The innermost point on 21Si is (312 ± 2) nm, the outermost on 25Si is (289 ± 2) nm. This yields a total difference of 23 nm corresponding to about 8%. Only silicon samples from the 'ring', i.e. samples 1Si to 20Si were used for the Round Robin experiment. The refractive index of the layers is about 1.90 and the mass density, calculated from the thickness and the ion beam analyses, is about 1.6 g cm^{-3}.

3. Analysis

The silicon samples allowed also to measure the thickness and the carbon content of the a-C:D deposits, in addition to the deuterium content. The carbon content of the a-C:D deposits could not be measured on the carbon samples, but they allowed, on the other hand, thermal desorption measurements of the deposits up to temperatures of 2000 K.

The deuterium content of the samples was measured at six laboratories by different experimental techniques:

- At Max-Planck-Institut für Plasmaphysik (IPP), Garching with the D(^{3}He,p)α NRA, using 790 keV ^{3}He ions [18,44] (Section 3.2) and by ERDA using 2.6 MeV incident ^{4}He ions and detecting the recoils in a surface barrier detector with a stopper foil in front of it to absorb the backscattered ^{4}He [19,45] (Section 3.4.1).
- At Beschleuniger Laboratorium, Garching with ERDA, by Section Physik, Ludwig-Maximilians-Universität München (LMU) and by Physik Department E12, Technische Universität München (TUM) Section Physik.
  At Section Physik, Ludwig-Maximilians-Universität München (LMU), 210 MeV ^{127}I ions were used. The heavy recoils were detected with an ionisation chamber [46] and the light recoils with a 'gas-semiconductor telescope' [26,34] (Section 3.4.2).
  At Physik Department E12, Technische Universität München (TUM), 80 MeV ^{197}Au ions were used and the recoils were analysed using a gas–semiconductor ΔE–E telescope [47] for standard elemental analyses and the charged recoils were analysed with a Q3D magnetic spectrograph for high resolution analyses [47] (Section 3.4.2).
- At Institut für Ionenstrahlphysik und Materialforschung, Forschungszentrum Rossendorf, Dresden, by ERDA, using 35 MeV ^{35}Cl ions and detecting the heavy recoils with a Bragg ionisation chamber [48] and the light recoils with a 'semiconductor telescope' [26] (Section 3.4.3). One sample was further analysed by calibrated negative SIMS (Section 4).
- At Max-Planck-Institut für Plasmaphysik, Bereich Berlin, by thermal desorption spectrometry (TDS) and by positive SIMS (Sections 4 and 5).
- At Institut für Experimentelle Physik, Abteilung Vakuumphysik und-technik, Otto-von-Guericke-Universität Magdeburg, by temperature programmed thermal desorption spectrometry (TPD) [31] (Section 5).

3.1. Sample characterisation

All samples used for the Round Robin investigations were analysed at IPP, Garching, prior to their shipment to the different groups, employing the D(^{3}He,p)^{4}He NRA at 790 keV incident energy, to verify the homogeneity of the deuterium content in the deposited layers (see Section 3.2). On each sample three spots with a size of 1×1 mm^2 were analysed with a charge of 0.2 μC per spot. This fluence of 1.3×10^{14} ions cm^{-2} is low enough so that the ion-induced desorption of deuterium [19] is within the statistical errors of the measurement. The number of detected protons created in the nuclear reaction was $>10^4$ for each spot, resulting in a statistical counting error of <1%. Although the error in the determination of the absolute amount of D is larger (see Section 3.2, below), the error in comparing the samples relative to each other is only given by the statistical error. The average value of deuterium in the a-C:D layers for the carbon samples (C samples) and separately for the silicon samples (Si samples) was computed from measurement at three spots on each sample. The a-C:D layers, which had been deposited onto the carbon

samples, yielded an average value of 175×10^{16} D atoms cm^{-2}, with a standard deviation of the samples from this mean values of ±2.5%. The maximum deviation of individual spots on the samples from the mean value was 3.5%. For the a-C:D layers deposited onto the silicon samples placed on the ring around the C samples (1Si to 20Si) the average value was lower by about 13%, i.e. 154×10^{16} D atoms cm^{-2} with a standard deviation of ±1.4% and a maximum deviation of ±2.2%. The D measured on the four silicon samples located inside the ring (21Si to 24Si) was higher by 4.2%, and on sample 25Si which was outside the ring it was lower by 4.2%. The gradient of the deuterium content from samples 21Si to 25Si was found to be in good agreement with the thickness gradient across these samples (see Section 2). The lower D content on the Si samples can therefore be partially explained by the observed deposition profile. The thickness profile and the deuterium content showed an increase of about 4% for the silicon samples 21Si to 24Si, which were placed closer to the centre of the electrode. We found, however, no indication for a further increase of the film thickness towards the centre, neither from the optical inspection of the interference colour of the carbon samples nor from the above described ion beam analysis. Therefore, the observed thickness gradient can account at most for about 5% deviation. The remaining deviation between the carbon and silicon samples of about 8% could be in principle due to a higher sample temperature during deposition because of insufficient clamping, but as discussed above (Section 2) this is not considered to be the reason for the observed difference. A possible explanation is that the silicon substrates were perfectly flat, while even the polished carbon substrates showed a surface roughness. Therefore the carbon samples posed a higher effective surface area, so that more material has been deposited onto them.

3.2. Nuclear reaction analysis

The cross-section for the D(^{3}He,p)α nuclear reaction has a broad maximum at incident ^{3}He energies of about 640 keV in the laboratory system and it is known to be 800 mb with an absolute accuracy of about 2% [18,49]. The cross-section is angle independent in the centre-of-mass system for incident energies below 1 MeV [49]. We have used incident ^{3}He ions with a slightly higher incident energy of 790 keV, resulting in an about uniform sensitivity for depths up to a few 100 nm. The protons created in the nuclear reaction were counted with a large acceptance angle (about 0.1 sr) surface barrier detector covered with a 0.1 mm stainless steel foil to stop the 3.5 MeV ^{4}He ions from the nuclear reaction, as well as the backscattered ^{3}He ions of the incident ion beam. The total ^{3}He ion beam charge used for each data point was 0.2 μC, as measured by a Faraday cup. Additionally, for calibration of the large acceptance angle proton counter a thin D-implanted erbium layer was used and in addition the spectrum of the backscattered ^{3}He including the α-particles from the nuclear reaction were recorded at a scattering angle of 165° by a surface barrier detector with a small opening angle of 1.08×10^{-3} sr ±2%. The total charge of the incident ^{3}He ion beam used for this analysis was 5 μC ± 5%. The large acceptance angle proton counter could therefore be calibrated with the 165° detector, resulting in the same inaccuracy of about 2% for the solid angle. The energy loss of the incident ^{3}He particles in the deposited a-C:D layers was about 96 keV. The change of the cross-section from 790 to 690 keV is about 15% and was taken into account. The absolute errors of both measurements due to errors in current integration, solid angle determination and uncertainties in the cross-section are about 6%. The statistical errors due to the number of counts is <1% for the measurements with the large angle proton counter and <3% for the 165° detector. The average values obtained by the NRA analyses of all a-C:D layers deposited on 20 carbon and 11 measured silicon samples, which had been performed before shipping the samples to the different laboratories, are shown in Table 3.

3.3. Proton elastic backscattering

The a-C:D layers on Si samples have also been analysed by elastic backscattering of 1.5 MeV H^+. The protons hit the surface at normal incidence and the backscattered protons were detected at a scattering angle of 165°. The incident flux was measured with a Faraday cup. Two peaks, one of D and one of C in the a-C:D layer were found in the backscattering spectrum (Fig. 2). However, only the C peak was evaluated due to the unknown cross-section for scattering of 1.5 MeV

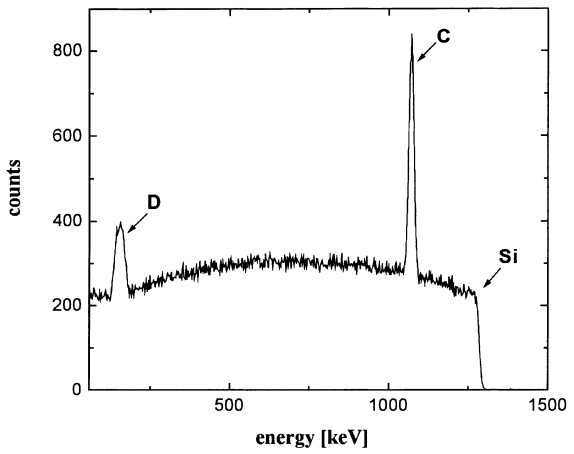

Fig. 2. Spectrum of backscattered protons from the a-C:D layer on silicon sample 3Si.

protons at D [50]. The values for carbon are included in Table 3.

3.4. Elastic recoil detection analyses

The surface layer to be analysed is bombarded with keV to 100 MeV ions. Atoms from the layer are scattered by binary elastic collisions with the incident ions. The recoil atoms leaving the surface at a shallow angle with respect to the surface are analysed for their mass and energy, the latter is correlated to the depth from which the recoils are generated [19,51]. Absolute amounts and depth profiles of D can be calculated from the analysing ion fluence and from the number and energy of the recoils detected within a known acceptance angle of the detector [47–51], using the Rutherford scattering cross-section and tabulated stopping powers for the ions in solids [52].

3.4.1. ERDA with light ions (Max-Planck-Institut für Plasmaphysik, Garching)

In the ERDA measurement at IPP for the hydrogen isotopes an ion beam of 2.6 MeV ^{4}He was used with an angle of incidence of 75°. The detector was placed at an exit angle of 75° with respect to the surface normal, corresponding to a recoil angle of 30°. The beam spot area on the target surface was 2×1 mm^2. A total charge of 1 μC was used, as measured by a Faraday cup, corresponding to about 6×10^{12} ^{4}He ions or a fluence of 3×10^{14} ^{4}He ions cm^{-2}. The detector had a solid angle of about 5×10^{-3} sr and was covered with a 5 μm stainless steel foil to stop backscattered ^{4}He ions and to allow only the hydrogen isotope recoils to enter the detector. The D(^{4}He,D)^{4}He recoil cross-section is 'non-Rutherford' at this energy [53], and the values measured and reported by different groups show large differences [53–55]. In order to avoid the problems associated with the uncertainty of the cross-section, the D content was determined against the known D content of a calibrated target ($9.8 \times 10^{17} \pm 10\%$ D atoms, implanted in Er). The energy losses of the incident ^{4}He ions in the a-C:D layers and in the implanted Er layer are nearly the same, therefore allowing direct comparison the number of counts. The absolute error is only determined by the accuracy of the calibrated target being about 10%. The results of the analysis are shown in Table 3. For the carbon sample 27C the value measured by ERDA was found about 7% higher than the mean value of the analysis, while the value for the carbon sample 32C was found about 6% lower.

3.4.2. ERDA with heavy, 210 MeV ^{127}I and 80 MeV ^{197}Au ions (Beschleuniger-Laboratorium, Garching)

At Beschleuniger-Laboratorium in Garching two different ERDA set-ups were used for the analyses. The use of heavy ions, which are not scattered into the detectors by the elements present in the samples means that the stopper foil in front of the detectors could be avoided in both cases:

In one experiment, performed by Ludwig-Maximilians-Universität, München, 210 MeV ^{127}I ions were used, at an angle of incidence of 71.2° relative to the surface normal and the detector symmetrically to the incidence conditions, i.e. a scattering angle of 37.6°. The detector covered a solid angle of about 6 msr. The recoil atoms, with the exception of hydrogen, were analysed using a ΔE–E telescope. This consists of an ionisation chamber where the anode, by which the charges are extracted, is divided into two parts. The charge from the smaller anode at the entrance gives the ΔE signal for identifying the recoiling particles, while the charge extracted from the first and the second electrodes gives the E signal [46]. The raw data measured for the a-C:D layer on the Si sample 11Si are shown in Fig. 3. The a-C:D deposition is found to contain about 0.3% oxygen and nitrogen; the silicon substrate is also seen at larger depths. The recoiling hydrogen isotopes are generally not stopped in the ionisation chamber and are analysed

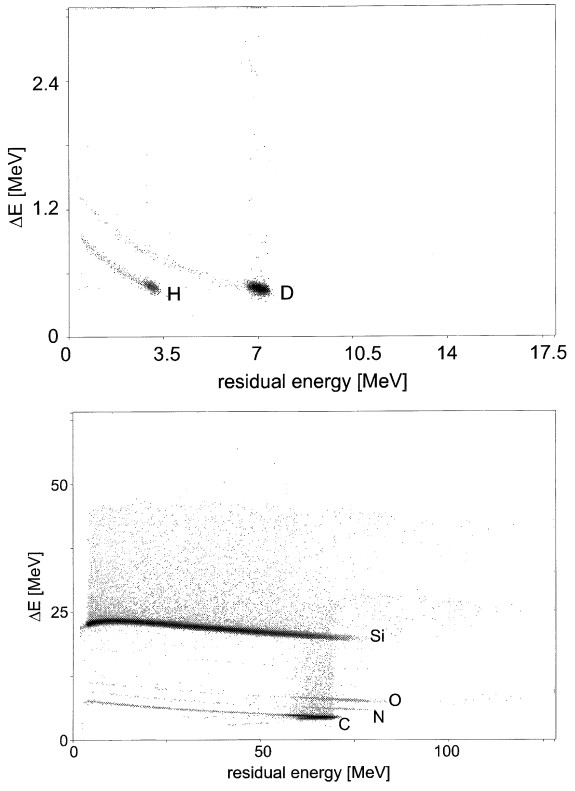

Fig. 3. Two-dimensional plot of the ERDA signals as measured with 210 MeV ^{127}I ions for an a-C:D layer on silicon sample 11S. The upper figure shows the ERDA recoils D and H. The lower figure shows the ERDA signals from C and Si, as well as from N and O, being present at small concentrations.

using a silicon surface barrier detector situated at the end of the chamber. This covers an opening angle of about 1 msr. In order to separate the different hydrogen isotopes the ΔE signal is taken from the charges created by the hydrogen isotopes in penetrating the total length of the ionisation chamber. The analysis shows that the a-C:D layer contains in addition to D also some H. The signals of D and H are well separated (see Fig. 3). Integration of these signals allows to determine the total amount of the hydrogen isotopes in the a-C:D layers if the ion analysing charge is known. This charge was calculated from the ERDA intensity of the simultaneously measured Si substrate.

In the ERDA measurements especially with high atomic mass ions, a relatively strong bombardment-induced desorption of the hydrogen isotopes was found, which can introduce larger errors in the results [34]. The decrease of the deuterium ERDA signal with analysing fluence for the 210 MeV ^{127}I ions used in the analysis by LMU, München, is shown in Fig. 4. This decrease was fitted to the predicted analytical dependence of the decrease with incident fluence [35]. The extrapolation to zero analysing fluence resulted in a total amount of 150×10^{16} D atoms cm^{-2}, the value was taken for Table 3.

The second analysis was performed with the set-up at TU, München. In this case 80 MeV ^{197}Au ions were used. Compared to the 210 MeV ^{127}I ions they have a much higher scattering cross-section due to the higher atomic number and the lower energy. For analysing the hydrogen isotopes, a hybrid ΔE–E detector was used which consisted of a ΔE-gas detector and a residual energy solid-state detector with an acceptance angle of 6 msr. The angle of incidence was 82° to the surface normal and the detector was mounted at an angle of 57.6° to the surface normal, corresponding to a scattering angle of 40.4°. The measured raw data gave a plot, similar to Fig. 3. The total amount of D and H in the a-C:D layers is obtained by integration of the D and H recoil intensities, respectively. The higher sensitivity for 80 MeV ^{197}Au ions, as compared to 210 MeV ^{127}I ions, allowed to use about a factor of 100 lower incident fluences for the analyses. For these low fluences nearly no bombardment-induced D desorption was observed within the statistical uncertainties, i.e. the measured deuterium content remains about constant up to the analysing fluences of about 8×10^9 ^{197}Au ions cm^{-2}. The data are plotted in Fig. 5. They yield a total amount of about 200×10^{16} D atoms cm^{-2}. Due to the higher sensitivity, the larger number of detected counts resulted in small statistical errors (<2%). The D/C ratio was calculated to be 0.775 ± 0.002. Note that the analyses with 210 MeV ^{127}I ions started only at higher fluences, i.e. at a fluence $>3\times10^{10}$ ^{127}I cm^{-2}. The electronic stopping powers, causing the hydrogen isotope release, are nearly the same for 210 MeV ^{127}I and 80 MeV ^{197}Au ions, therefore, to a first-order approximation, the fluence can be scaled to the damage production and the hydrogen release using the same factor.

Calibration of the deuterium content was performed by calculating from the raw data the depth profiles for the relative amounts of all elements in the samples using the computer code KONZERD [56]. The energy calibration of the ΔE–E detector, the values for the stopping power for ^{179}Au ions in the Si backing and the scattering geometry have to be known for the determination of the absolute amount of deuterium from the measured spectra. Due to the rather low energies of the recoils, an accurate energy calibration of the detector was not possible for this first experiment. The stopping power values calculated by the computer simulation program TRIM may differ from the real values by up to 20%. The angle of the impinging ^{179}Au ions was only known with an accuracy of $\pm0.5°$. From these uncertainties in the experimental parameters an uncertainty of about 25% resulted for the determination of the absolute amount of deuterium,. The obtained depth profiles for C and D as

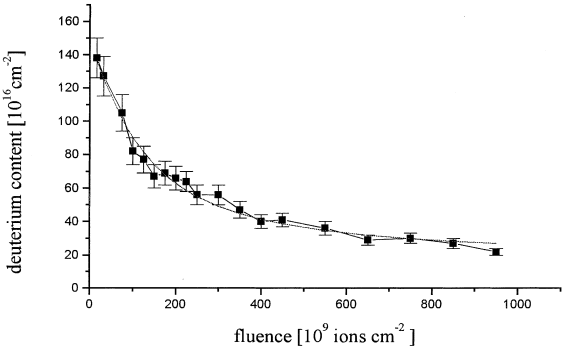

Fig. 4. Decrease of the D signals with ion fluence in an ERDA measurement for an a-C:D layer on silicon sample 11Si, using 210 MeV ^{127}I ions.

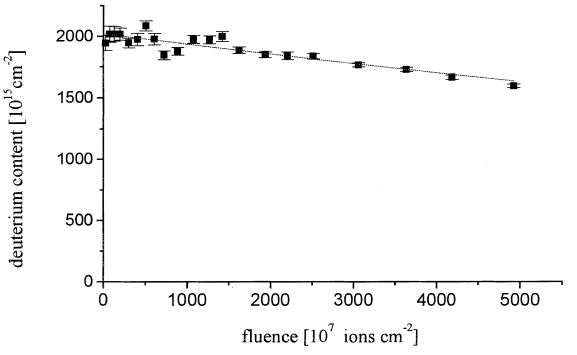

Fig. 5. Decrease of the D signals with ion fluence in an ERDA measurement for an a-C:D layer on silicon sample 12Si using 80 MeV ^{197}Au ions.

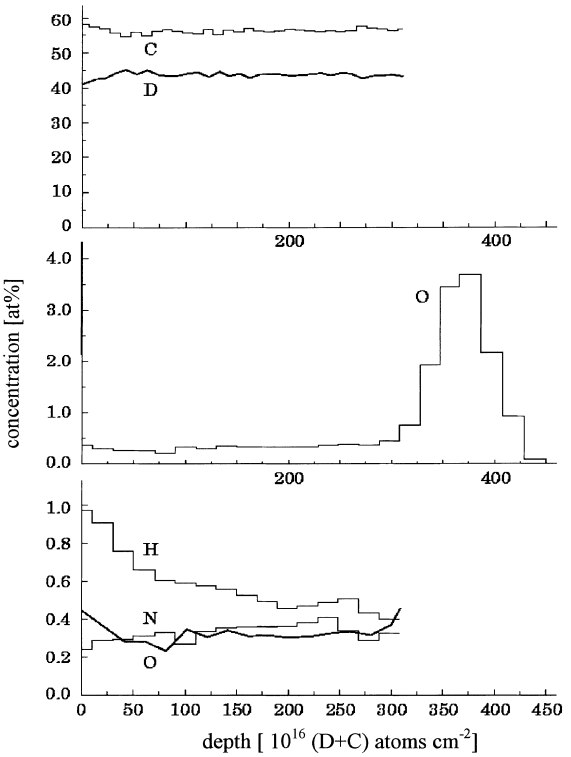

Fig. 6. Depth profiles of O, H, N, C and D as measured in an ERDA analysis for an a-C:D layer on silicon sample 12Si, using 80 MeV ^{197}Au ions.

well as for the impurities H, N and O are shown in Fig. 6. The accuracy of the depth profiles by use of this calibration was estimated to be 7% mainly due to the uncertainty in the stopping power of the ^{179}Au ions in Si. The accuracy of the integrated D/C ratio does not depend on stopping powers; due to the well-known Rutherford cross-section it is only limited by statistics. The accuracy of this ratio is better than 1% in case of the 80 MeV ^{179}Au ions. The thickness of the a-C:D layer can be further estimated from the depth of the oxygen peak (Fig. 6). Based on the known D concentration it is also possible to determine the amount of deuterium in the a-C:D layer. The value which was obtained is lower by about 25%, and it was also included in Table 3.

In the analyses with 80 MeV ^{179}Au ions, the deuterium depth profile was further simultaneously measured with high energy resolution, i.e. high depth resolution at a scattering angle of 15° using the Munich Q3D magnetic spectrograph. The profile of an a-C:D layer on a Si sample is shown in Fig. 7. Only a surface layer corresponding to the first 70×10^{16} atoms cm^{-2} was measured due to the limited acceptance angle of the Q3D. Except for a small deuterium peak at the front of the sample, the profile was found to be constant within the error bars. The thickness of the surface layer with the high D

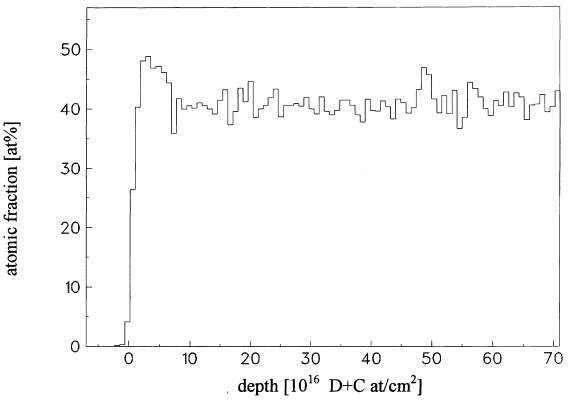

Fig. 7. Depth profile of D in an a-C:D layer on a silicon sample as measured with the high resolution Q3D showing the very uniform depth distribution, except for a slight surface peak.

concentration on the a-C:D layer is about 3 nm FWHM and it is the region where the ions have penetrated the film in the last step of deposition. The additional deuterium content in the peak is much less than 1% of the total deuterium content of the a-C:D films.

3.4.3. ERDA using 35 MeV ^{35}Cl ions (Forschungszentrum Rossendorf)

In the ERDA at Forschungszentrum Rossendorf, a primary ion beam of 35 MeV $^{35}Cl^{7+}$ ions from the Rossendorf tandem accelerator was hitting the sample at an angle of 75° relative to the surface normal with a beam spot area of 3×1 mm^2. The energetic recoiling H and D ions created at an angle of 38° and leaving the surface at 67° with respect to the surface normal were detected with a semiconductor telescope detector, having a 16 μm thick Al foil in front to stop all scattered ^{35}Cl ions [26]. The heavier recoiling target atoms were detected with a Bragg ionisation chamber at a recoil angle of 30°, i.e. at an angle of 75° with respect to the surface normal [26,48]. The acceptance angles of the detectors were determined by the geometry as well as by measuring of standards, giving an opening angle of 2.13 msr ±5% for the semiconductor telescope and 0.42 msr ±5% for the Bragg ionisation chamber. The measured recoil spectra for H, D, O, and C are shown in Fig. 8, while Fig. 9 shows the depth distributions evaluated from the measurements. For sample 23C, the total amount of deuterium measured in this analysis was corrected for deuterium release during the measurement (see Fig. 10). Due to the lower sensitivity in the use of ^{35}Cl ions larger fluences had to be used compared to the ERDA measurements with ^{127}I ions and ^{179}Au ions. This resulted in a larger bombardment induced D release. Extrapolation to zero analysing fluence gave a deuterium content of 145×10^{16} Dcm^{-2}, i.e. about a factor of 8

higher deuterium content than measured at the end of the analysis (see Fig. 10). The value obtained by this extrapolation is included in Table 3. The deuterium amount in the Si sample 8Si was measured with an analysing fluence of 2×10^{13} ^{35}Cl ions cm^{-2} and has not been corrected for the deuterium release during the analyses. This number represents a lower limit, which may

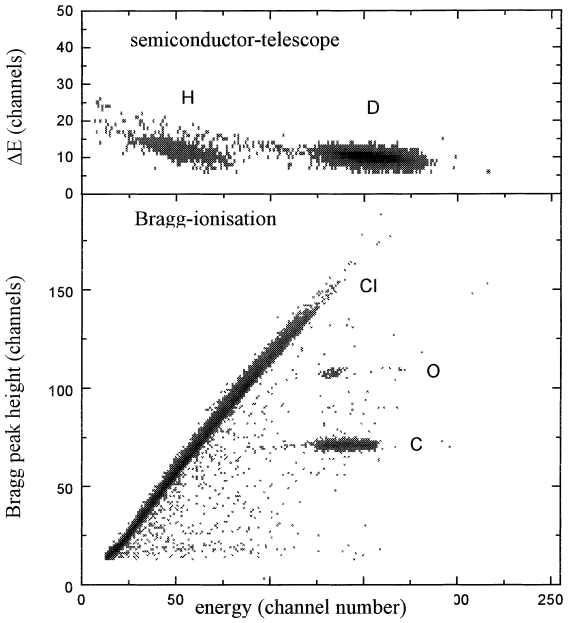

Fig. 8. Two-dimensional plot of ERDA signals as measured with 35 MeV ^{35}Cl ions for the a-C:D layer on silicon sample 13Si. The upper figure shows the ERDA recoils from D and H, the lower figure shows the ERDA signals from the C and O, being present at low concentrations. For the units of the energy and Bragg height peaks just the channel numbers of the multichannel analyser are given.

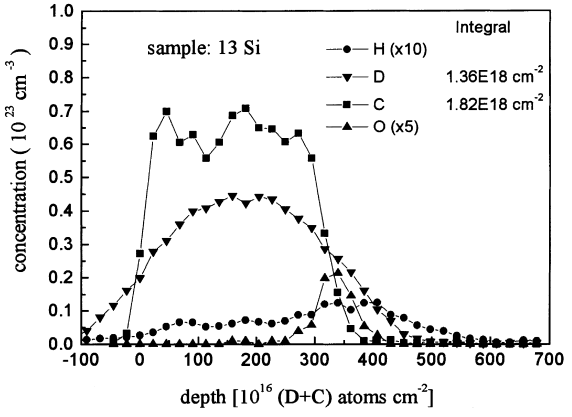

Fig. 9. Depth profiles for C, D, H and O, as deduced from ERDA spectra measured with 35 MeV ^{35}Cl ions measured on the silicon sample 13Si.

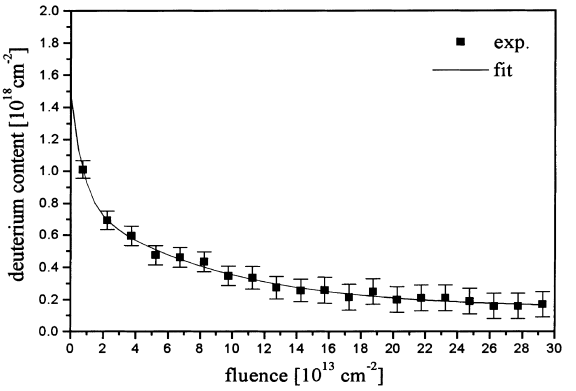

Fig. 10. Decrease of the D signals with ion fluence in an ERDA measurement for an a-C:D layer on carbon sample 23C using 35 MeV ^{35}Cl ions.

have to be increased by a factor of about 1.6. This is not taken into account in Table 3.

4. Secondary ion mass spectrometry (Forschungszentrum Rossendorf)

SIMS measurements were performed with the negative secondary ions formed at the injector ion source of the AMS set-up in Rossendorf [29]. Samples cut to a diameter of about 5 mm were installed as the target in the negative ion source. They were bombarded with 5 keV Cs^+ ions and the sputtered D^- ions were extracted, mass analysed with the injection sector magnet and measured in a Faraday cup behind the magnet. In order to avoid the effects occurring at the sides of the sputtered crater, the target was mechanically scanned and the sputtered ions were recorded only when the sputtering Cs ions hit at the centre of the crater on the target [29]. This set-up was calibrated with D-implanted carbon samples. The total amount of D and the depth distribution were calculated from the calibrated SIMS signals (Fig. 11) and the depth of the crater measured after the analysis using a micro profilometer [29,30]. The results are shown in Table 3; they are about 20% higher than the mean values.

In the SIMS analysis performed at IPP, Bereich Berlin, only the thickness of the deposited layer was measured and found to be 220 nm (see Table 3).

5. Thermal desorption measurements

TDS or TPD measurements were performed at Institut für Experimentelle Physik, Abteilung Vakuumphysik und-technik, Otto-von-Guericke-Universität Magdeburg and at IPP, Bereich Berlin.

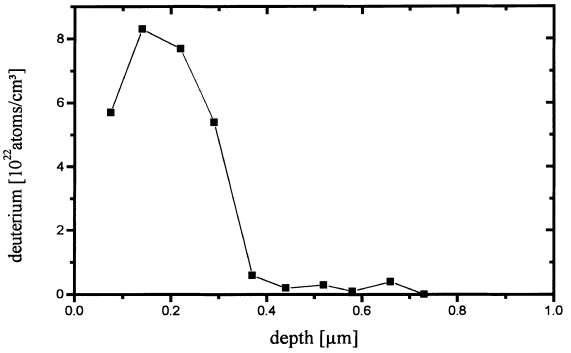

Fig. 11. Negative SIMS depth profile of D measured at the AMS injector in Rossendorf for an a-C:D layer on silicon sample 28Si using Cs ions.

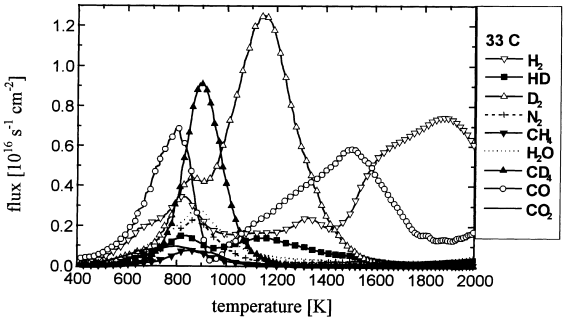

Fig. 12. Temperature programmed desorption (TPD) spectra measured for the a-C:D layer on carbon sample 33C for a heating rate of 10 K s^{-1}. (The total amounts of the desorbed gases are summarised in Table 2.)

5.1. Universität Magdeburg measurement

At Universität Magdeburg temperature programmed desorption (TPD) measurements were performed in an UHV system having a volume of about 1.5 l, with an ultimate pressure in the 10^{-9} mbar range. After mounting the sample onto the holder and into the vacuum chamber, the system was baked at 400 K for about 16 h. After cooling down, the QMS and the tungsten filament which was used for heating the sample by electron bombardment from the rear, were degassed, the current of the tungsten filament was increased up to the final value in a time of about 10 s. At the end of the resulting short pressure rise the acceleration voltage was applied to the sample, which was electrically insulated with respect to the chamber walls. The voltage was increased up to 1000 V so that the samples were uniformly heated by the electron bombardment from the rear side. The voltage was programmed to result in a linear temperature increase at a rate of about 10 K s^{-1} up to temperatures of 2100 K. The temperature was measured at the front side of the sample by a pyrometer placed outside the vacuum chamber using a UHV viewing port made of magnesium fluoride. The partial pressures were determined with a quadrupole mass spectrometer (QMS) [31]. In order to get quantitative results, the QMS was calibrated by filling the chamber with purified gases and measuring the pressures with a spinning rotor gauge taking into account the different sensitivities for different masses. During the TPD analyses the ion currents in the QMS were measured as a function of the sample temperature [31]. The fluxes of desorbing gases were calculated taking into account the sensitivities of the QMS and the device parameters such as the volume and the effective pumping speed. The desorbed fluxes for the carbon sample 33C plotted as a function of the linearly rising target temperature are shown in Fig. 12. The inventories were calculated by integrating the fluxes of the different D containing species emitted over the whole temperature range. The results for all desorbed species are shown in Table 2, the results for the total amount of D are also included in Table 3. Only about half of the deuterium was released as D_2, the other fraction was released as CD_4 and some DH. The measured relative high contribution of CD_4 indicates that higher hydrocarbon components have also been likely released from the a-C:D films. Higher masses, such as C_2D_5 (mass 34) and C_2D_6 (mass 36) have been seen in test measurements, however, the signal height of the QMS had not been calibrated for the higher masses. A rough estimation gave a contribution of the higher hydrocarbon molecules to the released D of about 20%. Unfortunately, this contribution could not be quantified in the present experiment. However, it should be included in order to get reliable measurements. After each degassing, the heating was repeated, but the measured fluxes were found to be about a factor 100 lower. The relatively large amount of measured H, particularly at high sample temperatures, may have been due to heating and degassing of the walls of the vacuum chamber.

Table 2
Total amounts of H and D and of all measured desorbed species for temperature programmed desorption (TPD) of the carbon sample 33C by heating from 273 to 2016 K

Desorbed species	Total inventory [$\times 10^{16}$ cm^{-2}]
H-(total)	136
D-(total)	119
H_2	61
HD	8.11
D_2	32.9
N_2	6.1
CH_4	1.49
H_2O	7.88
CD_4	11.2
CO	42.7
CO_2	3.7

5.2. Measurements at IPP, Bereich Berlin

The TDS measurements at IPP, Bereich Berlin, were carried out in a UHV system, having a volume of 40 l, which allowed to perform desorption measurements of relatively large samples with a size up to $100\times 100\times 10$ mm^3 [8,9]. It consisted of two chambers. The larger main vessel was pumped by a turbomolecular pump with a pumping speed of 200 l s^{-1} for hydrogen, giving a base pressures of $<10^{-6}$ Pa. The samples to be analysed were put onto a molybdenum holder and were heated by electron bombardment with constant heating power, resulting in non-linear heating rates. Temperatures above 2000 K were achieved after a heating time shorter than 60 s. A fraction of the desorbed gas reached the analysing chamber through a flow conductance of 1 l s^{-1}. This chamber was pumped by another turbomolecular pump down to pressures of $<10^{-6}$ Pa. It was equipped with a quadrupol mass spectrometer for analysing the desorbed gases. Calibration of the QMS was performed by introducing purified gas into the desorption chamber and the total pressure was measured with an ionisation gauge. The calibration was checked by degassing a deuterium containing carbon layer on a tungsten sample whose amount of deuterium had been previously measured by NRA [8,9]. In order to determine the desorbed deuterium fluxes, the temporal evolution of the partial pressures of D_2, HD and CD_4 were measured. The total deuterium inventory of the samples was determined by integrating the fluxes of these molecules over the whole heating time. The contribution of other deuterium containing species was neglected. The results are included in Table 3.

6. Discussion

The results for the absolute amounts of D in the a-C:D layers, which were determined independently in the measurements at the six laboratories, are summarised in Table 3. The first row gives the average values for the amount of deuterium determined by the D(^{3}He,p)^{4}He nuclear reaction (Section 3.2) measurements of all 20 carbon and 11 silicon samples from the ring before shipping them to the different laboratories. The reasons for the difference of the values between carbon and silicon samples were already discussed in Section 3.1. The following rows give the experimental values obtained for the individual samples by the different groups with their own methods. The last row gives mean values for the C and Si samples calculated by adding the individual results and dividing them by the number of measurements, as discussed in the following.

The total uncertainty of each experimental result yielding an absolute number is determined by statistical and by systematic errors. The statistical error arises from counting statistics and experimental uncertainties due to a lack of control over certain parameters. The systematic errors are due to, for example, incorrect calibration of measuring instruments, errors of cross-sections used for data analysis, or incorrect measurement of experimental parameters such as scattering angle, detector solid angle, or analysing ion beam fluence. The statistical error may vary from measurement to measurement or sample to sample in the same set-up. It can be reduced by repeating the measurements and averaging. On the other hand, the systematic error is the same for each measurement and gives rise only to a scaling of the result, but maintaining the relative value. This means, if the results of two measurements at two different samples using the same set-up and analysis method differ by some factor, this must be due to different amounts on the samples and the measured results will always differ by the same factor. This does not depend on the absolute values and may be due to, for example, the use of an incorrect cross-section. In this sense, we can consider the initial analysis of the complete set of carbon samples and the 11 analysed silicon samples described in Section 3.1 as a proof of the homogeneity of the deposits without making conclusions about the total precision of the applied method. Because the hydrogen isotopes are very strongly bound in these layers, their amount does not change in the time between the initial NRA analysis and the analyses in the different laboratories.

Deviations between the measurements of different groups or different methods are significantly larger than the found standard deviations of about 2.5% for the carbon and 1.5% for the silicon samples and cannot be due to differences in the samples. Since the main purpose of this work is to compare different quantitative methods with each other, it was implicitly assumed that the differences between the results of the different methods are not governed by statistical errors, but due to systematic errors. Care should be taken to assure that each method enters the calculation of the mean value with the same statistical weight. Therefore, we first calculated the algebraic mean of the results of the same method, if more than one sample was measured with this method, and then took this value to calculate the algebraic mean of the different methods. Accordingly, the average of each of the two measurements for samples 27C and 32C, of 18Si and 24Si, of 24C and 33C, and of 36C and 37C was used for the calculation of the mean value, since the same method was applied in these cases. According to this procedure, the mean value was calculated from 6 and 7 values for C-and Si-samples, respectively.

The mean values and standard deviations are $(159\pm 23)\times 10^{16}$ D atoms cm^{-2} for the carbon samples and $(149\pm 26)\times 10^{16}$ D atoms cm^{-2} for the silicon samples. Two observations become immediately apparent from these data. Firstly, the standard deviations of

Table 3
Amounts of deuterium and carbon as measured by different techniques at different laboratories for a-C:D layers deposited on carbon and silicon samples by low-pressure plasma deposition[a]

Analysis technique, laboratory	Sample number, material	Total D content $\times 10^{16}$ D cm^{-2} (difference to mean value %)	Total C ($\times 10^{16}$ C cm^{-2})	D/C ratio	Area density, thickness (nm) 1 nm $\approx 1.1 \times 10^{16}$ (D+C) cm^{-2} ($\rho_C \approx 6.7 \times 10^{22}$ C cm^{-3}, $\rho_D \approx 4.5 \times 10^{22}$ D cm^{-3})	Comments
Average values of the NRA analyses at	C	$175 \pm 2.5\%$ (+10)				Average over 20 carbon and 11
IPP before shipping to the different labs	Si	$154 \pm 1.4\%$ (+3.4)			300 ± 2 profilometer	silicon samples, respectively
NRA, 790 MeV ^{3}He, IPP, Garching (M. Mayer)	3Si	155 (−4)				Large angle detector, no extrapolation to zero fluence needed
1.5 MeV H^+ elastic backsc., IPP, Garching (M. Mayer)	3Si		218	0.71	300 ± 2 profilometer	$\Theta = 165^0$
ERDA, 2.6 MeV ^{4}He, IPP, Garching	27C	170 (+7)				$\Theta = 30^0$ no extrapolation to zero
(M. Mayer)	32C	150 (−6)				fluence
	18Si	129 (−13)				
	24Si	128 (−14)				
ERDA, 210 MeV ^{127}I, LMU, München (W. Assmann)	11Si	$150 \pm 7\%$ (+0.6)				$\Theta = 37.6^0$ (extrapol. to zero fluence)
ERDA, 80 MeV ^{197}Au, TU, München	12Si	$200 \pm 25\%$ (+34)				$\Theta = 40.4^0$, (extrapol. to zero fluence)
(G. Dollinger et al.)		150 (+0.6)	190	0.78	340×10^{16} (D+C) cm^{-2}	From O peak on Si
ERDA, 35 MeV Cl, FZ Rossendorf	23C	145 (−9)				$\Theta = 38^0$ (extrapol. to zero fluence)
(U. Kreissig)	8Si	123 (−17)	169	0.73	330×10^{16} (D+C) cm^{-2}	Not corrected for depletion
	13Si	137 (−8)	182	0.75	320×10^{16} (D+C) cm^{-2}	From O peak on Si
Neg. SIMS (Cs sput.), FZ Rossendorf (M. Friedrich, G.Y.Sun)	28C	191 (+20)		<0.8	$\leqslant 350$	Calibrated with implanted samples
TPD (temperature programmed	24C	132 (−17) [b])				55% as D_2, 38% as CD_4 7% as HD [b])
desorption) Uni Magdeburg	33C	119 (−25) [b])				
(D. Schleußner et al.)						
TDS, IPP, Berlin (D. Hildebrandt et al.)	36C	163 (+3)				77% as D_2, 10% as HD 13% as CD_4
pos. SIMS	37C	149 (−6)				
	34C			0.7	220	From crater depth
Mean values of the analyses by the	C	159 ± 23 (= ±14.5%)				
different groups and techniques	Si	149 ± 26 (= ±17.5%)	190 ± 23	0.73 ± 0.2	323	

[a] The experimental uncertainties for some of the measurements as provided by the different laboratories are given in %. The values in parentheses give the difference to the mean values in %.
[b] Higher masses not included (+≈20%).

both sets are 14.5% and 17%, respectively. They are significantly higher than the standard deviations measured by only one method, which where 2.5% and 1.5% (Section 3.1). Secondly, the difference of about 13% between the average values for the silicon and carbon samples is not found in the mean values. Both points indicate that additional uncertainties enter the data evaluation. These are ascribed to systematic errors and discussed below.

The mean value of D for the C substrates is lower by about 10% than the average value determined by NRA for all samples prior to shipping. The low mean value of D for the a-C:D layers on carbon substrates may be due to the too low amounts of deuterium measured by TPD due to neglecting the release of higher mass hydrocarbons. For D in the a-C:D layers on silicon substrates, the mean value is only 3% lower than the average value determined by NRA for all samples prior to shipping. This may be due to those values which have not been corrected for depletion during the analyses.

The differences of the values of individual measurements to the mean value are given in parenthesis in column 3 of Table 3. For understanding the differences between the results measured by different techniques at different laboratories, the calibrations and uncertainties of each technique including possible systematic errors have to be considered.

In all measurements with MeV ion beams a possible common source of error is the measurement of the analysing ion fluence and the detector solid angle. In ERDA analysis additional sources of error are small uncertainties of the close to glancing angles of the incident ion beam and the detected recoils toward the sample surface, and the small scattering angles combined with the strong angular dependence of the Rutherford cross-section. Even a small misalignment of the sample surface with respect to the incident beam and the detector for measuring the recoils, may result in changes of the scattering and recoil angles. The scatter among the 2.6 MeV ^{4}He ERDA analysis results is mainly due to this problem.

Bombardment-induced deuterium release is a further major problem, especially for the analysis by heavy ion ERDA, while it is only a minor problem for analysis with swift He ions. Just one analysis is generally not sufficient. On the contrary, a large number of subsequent measurements is needed to allow extrapolation to zero analysing fluence. In the heavy ion ERDA measurement, the deuterium signal was measured as a function of the analysing fluence and extrapolated to zero fluence (Figs. 4, 5, and 10). This extrapolation has also several uncertainties. There may be a relatively large D release already at very low analysing fluences, which may depend on the properties of the sample analysed and cannot be observed for the fluences needed for the first analysis. However, as seen in Fig. 5 the release may also be very small for low analysing fluences. Further, the decrease of the IBA signal depends on the structure and properties of the deposited films and on the analysing current distribution [35], the current density and the charge and energy of the analysing ions. These effects have not yet been sufficiently investigated [57].

In the D(^{3}He,p)^{4}He NRA method, which was used as the reference analysis technique the analysing ion current was measured with a Faraday cup and the opening angle of the detector was determined with a calibrated D-implanted target (see Section 3.2). The uncertainties in the numbers are mainly due to statistical errors. According to earlier investigations [19] for the analysing fluence used here, ion-bombardment-induced deuterium release is within the statistical errors.

For the ERDA analyses at LMU, München with 210 MeV ^{127}I ions the extrapolation of the deuterium ERDA signals to zero analysing fluence is shown in Fig. 4. It was fitted to the predicted analytical dependence on the incident fluence [35] resulting in a value for the amount of D which deviates by less than a few per cent from the mean value (Table 3).

For the ERDA analyses at TU, München with 80 MeV ^{197}Au, due to the higher sensitivity [51] a factor of about ten lower analysing fluence could be used. No decrease of the deuterium ERDA signal with analysing fluence was observed within the measuring statistics up to fluences of about 8×10^9 Au cm^{-2} (Fig. 5). A slow nearly exponential decrease was found at higher fluences. The value for the amount of deuterium of 200×10^{16} cm^{-2} is higher by 31% than the mean value. This indicates a systematic error, which is probably caused by the uncertainty in the stopping power of the 80 MeV ^{197}Au ions in the Si substrate, which enters in the determination of the analysing fluence from the Si recoil intensity by the computer code KONZERD. The amount of deuterium was also obtained from the thickness of the a-C:D layer and the D to C concentration ratio, without requiring the stopping power of the 80 MeV ^{197}Au ions in Si. This value falls within 1.3% of the mean value of all measurements.

35 MeV ^{35}Cl ions were used in the ERDA measurements at FZ Rossendorf. The observed decrease of the deuterium ERDA signal with analysing fluence for carbon sample 23C is shown in Fig. 10. The value obtained by extrapolation to zero analysing fluence is given in Table 3; it is lower by 9% than the mean value for all measurements For sample 8Si the ERDA analysis was performed with a fluence of 1.8×10^{13} ^{35}Cl ions cm^{-2}. The decrease of the deuterium ERDA signals with analysing fluence was not recorded, and the value given in Table 3 represents therefore only a lower limit. It is 20% lower than the mean. The value for sample 13Si was obtained from the measured D/C ratio and the depth of the oxygen peak. This determination of the D amount is not influenced by the current measurement of the

analysing ion beam and deuterium release during the analysis. The obtained value is 11% lower than the mean value. In the SIMS analysis only the atoms sputtered as ions are detected. The fraction of hydrogen sputtered as ions depends on several parameters, such as the substrate material, impurities in the substrate as well as the concentration and the binding states of the deuterium in carbon [58,59]. This means that a calibration for hydrogen implanted in carbon may not give the correct results for hydrogen in a-C:D layers. The larger amount of deuterium measured in the SIMS analyses (+20%) may well be due to the fact that deuterium sputtered from deuterium implanted into carbon gives a lower ion yield than deuterium sputtered from an a-C:D layer.

Other uncertainties play a role in the TDS analyses at Otto-von-Guerike Universität, Magdeburg and at IPP, Bereich Berlin. In the TDS measurements at Magdeburg, the mass spectrometer used had been calibrated separately for gases of the low mass molecules being released during the desorption. The fractional contribution of high molecular weight molecules to the deuterium release was not included because the QMS was not calibrated for these masses. Furthermore, in order to reduce the background from gases at the vessel walls, the system had been baked for 16 h to 400 K before the TDS measurement. This baking temperature was kept low to avoid degassing from the sample to be measured. The major reason for the comparatively low amounts of deuterium measured by TDS, which are shown in Table 3, is probably the missing contribution of heavier molecules.

7. Conclusion

a-C:D layers about 300 nm thick had been deposited onto Si and on C samples. They have been analysed for the absolute amount of deuterium at several laboratories using different techniques. The results for the absolute numbers deviate mostly by less than about 10 at.%, from the algebraic mean value, which was calculated including all results. A maximum deviation of about 34 at.% was found. This is regarded as a reasonable agreement because very different techniques have been applied to determine the absolute values. The few larger deviations can be explained by uncertainties in the respective measurements, such as for example not well-known stopping powers of the analysing ions in the substrate material in ERDA or the disregard of higher mass hydrocarbons in TDS. In ion beam analysis a major problem is the measurement of the ion fluence used for the analysis, the opening angle of the detector as well as corrections with respect to the ion bombardment-induced release of hydrogen during the analysis. The bombardment induced gas atom release is smallest for NRA using the light ^{3}He ions at the relatively low energy of 790 keV. In the SIMS analysis the probability of emitting the desorbed and sputtered atoms as negative or positive ions depends on several parameters including the binding state of the hydrogen in the substrate. Calibrations should be performed for the actual material and for a hydrogen concentration and binding states which is similar to that which is finally analysed [58]. The calibration of the mass spectrometer, the volumes, the pumping speed, the desorption of D in different molecules, especially the higher hydrocarbon species, have to be taken into account in the TDS analysis. Regarding all these difficulties an absolute measurement of the deuterium content to better than about 10 at.% seems possible.

References

[1] J.L. Cecchi, S.A. Cohen, H.F. Dylla, D.E. Post (Eds.), Proceedings of the Symposium on Energy Removal and Particle Control in Fusion Devices, J. Nucl. Mater. 121 (1984).
[2] R. Behrisch, in: B. Coppi, G.G. Leotta, D. Pfirsch, R. Pozzoli, E. Sindoni (Eds.), Physics of Plasmas Close to Thermonuclear Conditions, Proceedings Course in Varenna, 27.8–8.9 1979, EUR FU BRU/XII/476/80, vol. 1, 1980, p. 425.
[3] R. Behrisch, Atomic and plasma-material interaction data for fusion, Nucl. Fusion 1 (Suppl.) (1991) 7.
[4] H. Verbeek, J. Stober, D.P. Coster, W. Eckstein, R. Schneider, Nucl. Fusion 38 (1998) 1798.
[5] R. Behrisch, J. Ehrenberg, M. Wielunski, A.P. Martinelli, H. Bergsåker, B. Emmoth, L. DeKock, J.P. Coad, J. Nucl. Mater. 145–147 (1987) 723.
[6] J.P. Coad, R. Behrisch, H. Bergsåker, J. Ehrenberg, B. Emmoth, J. Partridge, G. Saibene, R. Sartori, J.C.B. Simpson, W.M. Wang, J. Nucl. Mater. 162–164 (1989) 533.
[7] P. Franzen, R. Behrisch, C. García-Rosales, ASDEX Upgrade team, D. Schleußner, D. Rösler, W. Knapp, Ch. Edelmann, Nucl. Fusion 37 (1997) 1357.
[8] D. Hildebrandt, M. Akbi, B. Jüttner, W. Schneider, J. Nucl. Mater. 266–269 (1999) 532.
[9] M. Akbi, D. Hildebrandt, B. Jüttner, W. Schneider, Max-Planck Institiut für Plasmaphysik, Bereich Berlin, IPP Report No 8/15 1998.
[10] W. Jacob, W. Möller, Appl. Phys. Lett. 63 (1993) 1771.
[11] W. Jacob, M. Unger, Appl. Phys. Lett. 68 (1996) 475.
[12] P. Koidl, C. Wild, R. Locher, R.H. Sah, in: R.E. Clausing, L.L. Horton, J.C. Angus, P. Koidl (Eds.), Diamond and Diamond-Like Films and Coatings, NATO-ASI Series B, 266, Plenum, New York, 1991, p. 243.
[13] A. von Keudell, W. Jacob, Appl. Phys. Lett. 66 (1995) 1322.
[14] A. von Keudell, W. Jacob, J. Appl. Phys. 79 (1996) 1092.
[15] M. Saß, A. Annen, W. Jacob, J. Appl. Phys. 82 (1997) 1905.
[16] R.A. Street, Amorphous Hydrogenated Silicon, Cambridge University, Cambridge, 1993.
[17] J.F. Ziegler, C.P. Wu, P. Williams, C.W. White, B. Terreault, B.M.U. Scherzer, R.L. Schulte, E.J. Schneid,

C.W. Magee, E. Ligeon, J. L'Ecuyer, W.A. Lanford, F.J. Kuehne, H. Kamykowsky, W.O. Hofer, A. Guivarch, C.H. Filleux, V.R. Deline, C.A. Evans Jr, B.L. Cohen, G.J. Clark, W.K. Chu, C. Brassard, R.S. Blewer, R. Behrisch, B.R. Appleton, D.D. Allerd, Nucl. Instrum. and Meth. 149 (1978) 19.
[18] C.J. Altstetter, R. Behrisch, J. Bøttiger, F. Pohl, B.M.U. Scherzer, Nucl. Instrum. and Meth. 149 (1978) 59.
[19] J. Roth, B.M.U. Scherzer, R.S. Blewer, D.K. Brice, S.T. Picraux, W.R. Wampler, J. Nucl. Mater. 93–94 (1980) 601.
[20] J. Bøttiger, S.T. Picraux, N. Rud, Ion Beam Surface Layer Analysis, Plenum, New York, 1976.
[21] D. Grambole, F. Herrmann, R. Klabes, W. Hauffe, R. Behrisch, Nucl. Instrum. and Meth. B 68 (1982) 154.
[22] R.S. Blewer, Nucl. Instrum. and Meth. 149 (1978) 47.
[23] J. Tirira, Y. Serruys, P. Trocellier, Forward Recoil Spectrometry Application to Hydrogen Determination in Solids, Plenum, New York, 1996.
[24] B.G. Skorodumov, I.O. Yatsevitch, Nucl. Instrum. and Meth. B 64 (1992) 388.
[25] J.A. Sawicki, J. Roth, L.M. Howe, J. Nucl. Mater. 162–164 (1989) 1019.
[26] U. Kreissig, R. Grötzschel, R. Behrisch, Nucl. Instrum. and Meth. B 85 (1994) 71.
[27] V.M. Prozesky, C.L. Churms, J.V. Pilcher, K.A. Springhorn, R. Behrisch, Nucl. Instrum. and Meth. B 84 (1994) 373.
[28] Ch. Magee, S. Cohen, D. Voss, D. Brice, Nucl. Instrum. and Meth. 168 (1980) 383.
[29] M. Friedrich, G. Sun, R. Grötzschel, W. Bürger, R. Behrisch, C. García-Rosales, M.L. Roberts, Nucl. Instrum. and Meth. B 123 (1997) 410.
[30] G. Sun, M. Friedrich, R. Grötzschel, W. Bürger, R. Behrisch, C. García-Rosales, J. Nucl. Mater. 246 (1997) 9.
[31] D. Schleußner, W. Knapp, Ch. Edelmann, C. García-Rosales, R. Behrisch, J. Vac. Sci. Technol. A 17 (1999) 2785.
[32] K. Plamann, R. Behrisch, Nucl. Instrum. and Meth. B 129 (1998) 501.
[33] G. Dollinger, M. Boulmoudnine, A. Bergmaier, T. Faestermann, C.M. Frey, Nucl. Instrum. and Meth. B 118 (1996) 291.
[34] R. Behrisch, V.M. Prozesky, H. Huber, W. Assmann, Nucl. Instrum. and Meth. B 118 (1996) 262.
[35] R. Behrisch, W. von der Linden, U. von Toussant, D. Grambole, Nucl. Instrum. Meth. B 155 (1999) 440.
[36] A.P. Martinelli, I.G. Hughes, R. Behrisch, A.T. Peacock, in: Proceedings of the Eighteenth European Conference on Controlled Fusion and Plasmaphysics, Berlin 1991, Europhys. Conf. Abstracts, 15C III 153.
[37] I. Hughes, R. Behrisch, A.P. Martinelli, Nucl. Instrum. and Meth. B 64 (1992) 434.
[38] D. Grambole, F. Herrmann, W. Hauffe, R. Behrisch, Nucl. Instrum. and Meth. B 158 (1999) 647.
[39] P. Coad, M. Rubel, C.H. Wu, J. Nucl. Mater. 241–143 (1997) 408.
[40] M. Mayer, R. Behrisch, K. Plamann, P. Andrew, J.P. Coad, A.T. Peacock, J. Nucl. Mater. 266–269 (1999) 604.
[41] A. von Keudell, R. Hytry, W. Möller, Appl. Phys. Lett. 62 (1993) 937.
[42] A. von Keudell, A. Annen, V. Dose, Thin Solid Films 307 (1997) 65.
[43] A. Annen, R. Beckmann, W. Jacob, J. Non-Cryst. Solids 209 (1997) 240.
[44] C.J. Altstetter, R. Behrisch, B.M.U. Scherzer, J. Vac. Sci. Technol. 15 (1978) 760.
[45] M. Wielunski, M. Mayer, R. Behrisch, J. Roth, B.M.U. Scherzer, Nucl. Instrum. and Meth. B 122 (1997) 113.
[46] W. Assmann, P. Hartung, H. Huber, P. Staat, H. Steffens, Ch. Steinhausen, Nucl. Instrum. and Meth. B 85 (1994) 726.
[47] A. Bergmaier, G. Dollinger, C.M. Frey, Nucl. Instrum. and Meth. B 136–138 (1998) 638.
[48] R. Behrisch, R. Grötzschel, E. Hentschel, W. Assmann, Nucl. Instrum. and Meth. B 68 (1992) 245.
[49] W. Möller, F. Besenbacher, Nucl. Instrum. and Meth. B 168 (1980) 111.
[50] R. Amirikas, D.N. Jamieson, S.P. Dooley, Nucl. Instrum and Meth. B 77 (1993) 110.
[51] W. Assmann, J.A. Davies, G. Dollinger, S. Forster, H. Huber, Th. Reichelt, R. Siegele, Nucl. Instrum. and Meth. B 118 (1996) 242.
[52] J.F. Ziegler, J.P. Biersack, U. Littmark, The Stopping and Range of Ions in Solids, Pergamon, New York, 1985.
[53] A.J. Kellog, J.E.E. Baglin, Nucl. Instrum. and Meth. B 79 (1993) 493.
[54] V. Quillet, F. Abel, M. Schott, Nucl. Instrum. and Meth. B 83 (1993) 47.
[55] F. Besenbacher, I. Stensgaard, P. Vase, Nucl. Instrum. and Meth. B 15 (1986) 459.
[56] A. Bergmaier, G. Dollinger, C.M. Frey, Nucl. Instrum. and Meth. B 99 (1995) 488.
[57] M.P. de Jong, A.J.H. Maas, L.J. vanIJzendoorn, S.S. Klein, M.J.A. deVoigt, J. Appl. Phys. 82 (1997) 1058.
[58] B. Dischler, Amorphous Hydrogenated Carbon Films in: P. Koidl, P. Oelhafen (Eds.), E-MRS Symposia Proceedings, vol. XVII, Les Editions de Physique, Paris, 1987, p. 186.
[59] V.Kh. Alimov, A.E. Gorodetzky, A.P. Zakharov, J. Nucl. Mater. 186 (1991) 27.